Pharmaceutical nanotechnology

Quantitative and qualitative effect of gH625 on the nanoliposome-mediated delivery of mitoxantrone anticancer drug to HeLa cells

Emiliana Perillo [a], Emilie Allard-Vannier [b], Annarita Falanga [a], Paola Stiuso [c], Maria Teresa Vitiello [d], Massimiliano Galdiero [d], Stefania Galdiero [a],[**], Igor Chourpa [b],[*]

[a] Department of Pharmacy, DFM Scarl – University of Naples "Federico II", 80134 Naples, Italy
[b] Université François-Rabelais, EA 6295 «Nanomédicaments et Nanosondes», Tours F-37200, France
[c] Department of Biochemistry, Biophysics and General Pathology, II University of Naples, 80138 Naples, Italy
[d] Department of Experimental Medicine – II University of Naples, 80138 Naples, Italy

ARTICLE INFO

ABSTRACT

The present work investigates *in vitro* the delivery of the anticancer drug mitoxantrone (MTX) to HeLa cancer cells by means of polyethylene glycol (PEG) liposomes functionalized with the novel cell penetrating peptide gH625. This hydrophobic peptide enhances the delivery of doxorubicin (Doxo) to the cytoplasm of cancer cells, while the mechanism of this enhancement has not yet been understood. Here, in order to get a better insight into the role of gH625 on the mechanism of liposome-mediated drug delivery, we treated HeLa cells with liposomes functionalized with gH625 and loaded with MTX; functionalized and not liposome were characterized in terms of their physico-chemical properties and drug release kinetics. To quantify the MTX uptake and to study the subcellular drug distribution and interaction, we took advantage of the intrinsic fluorescence of MTX and of the fluorescence-based techniques like fluorescence-activated cell sorting (FACS) and confocal spectral imaging (CSI). FACS data confirmed that gH625 increases the total intracellular MTX content. CSI data indicated that when liposomes are decorated with gH625 an enhanced staining of the internalized drug is observed mainly in hydrophobic regions of the cytoplasm, where the increased presence of an oxidative metabolite of the drug is observed. The cytotoxicity on HeLa cell line was higher for functionalized liposomes within 4–6 h of treatment. To summarise, the MTX delivery with gH625-decorated nanoliposomes enhances the quantity of both the intracellular drug and of its oxidative metabolite and contributes to higher anticancer efficacy of the drug at the delay of 4–6 h.

© 2015 Elsevier B.V. All rights reserved.

1. Introduction

Cancer remains a leading cause of death in the western world. Cancer chemotherapies usually involve the use of cytotoxic molecules which kill highly proliferative cancer cells but also other proliferative cells in bone marrow, the gastrointestinal tract and hair follicles leading to common side effects such as compromised immune system, hair loss *etc.* (Dawidczyk et al.,

2014). Mitoxantrone (MTX) is a synthetic anthracenedione antineoplastic agent derived from the anthraquinone dye ametantrone (Dunn and Goa, 1996). It is structurally similar to the anthracycline agent doxorubicin (Doxo), both drugs having a planar aromatic ring structure which enables them to interact with DNA by intercalation between base pairs. MTX can inhibit the activity of nuclear enzyme DNA topoisomerase (II), interfere with RNA and cause the crosslink of DNA and strand breaks and produce reactive oxygen species. MTX is believed to lack cell cycle phase specificity because it has cytocidal effects both on proliferating and non-proliferating cells (Wiseman and Spencer, 1997). Similar to Doxo, its main side effect is cardiotoxicity; although also neutropenia, bone marrow suppression and secondary acute myelogenous leukaemia have been reported in patients treated

[*] Corresponding author. Tel.: +33 247367162.
[**] Corresponding author. Tel.: +39 812536642.
E-mail addresses: sgaldier@unina.it (S. Galdiero), igor.chourpa@univ-tours.fr (I. Chourpa).

with MTX (Kroger et al., 2003). However, MTX has been shown to produce free radicals to a much lesser degree than Doxo (Novak and Kharasch, 1985).

Actual treatments of cancer disease remains an elusive alternative, offering limited efficacy with extensive secondary effects as a result of severe cytotoxic effects in healthy tissues. The advent of nanotechnology brought the promise to revolutionize many fields including oncology, proposing advanced systems for cancer treatment. Drug delivery systems are amongst the most successful examples of nanotechnology and allow the reduction of unwanted side effects of systemic delivery, while increasing drug accumulation in tumours and improving the therapeutic efficacy. A delivery tool should transport the drug to the target cells not only with high efficacy, but also with minimal toxicity and immune response avoiding its degradation and entrapment in endosomes. The development of a broad range of nanoparticle platforms with the ability to tune size, composition and functionalities has provided a significant resource for nanomedicine.

Liposomes play a key role as drug carriers and represent a relatively simple form of nanovectors, especially for the delivery of antineoplastic drugs (Cui et al., 2008; Madni et al., 2014); in fact, they modify the pharmacokinetics and biodistribution of the drug, thus resulting in lower toxicity and higher efficacy. Liposomes are able to selectively deliver the drug into malignant areas due to enhanced permeability and retention effects (EPR). As a result, the exposure of healthy tissues to toxic drugs is reduced and therapeutic indexes are improved. Unfortunately, following intravenous injection, many nanoliposomes are easily recognised by the reticulo endothelial system (RES) resulting in rapid clearance and nonlinear pharmacokinetics. To reduce this effect, polyethylene glycol (PEG) has been introduced on the surface of liposomes. This modification is a milestone breakthrough in the field of drug delivery and is widely known as stealth technology. PEG-coated liposomes display a good pharmacokinetic profile and reduced systemic toxicity; however, their uptake in cells is delayed. In order to facilitate the interaction between liposomes and cells, the liposome surface can be functionalized with cell penetrating peptides (CPPs). CPPs have received much attention because of their ability to enable several kinds of cargoes to cross cell membranes both *in vitro* and *in vivo* (Heitz et al., 2009; Galdiero et al., 2014). CPPs are short and usually basic amino acid rich peptides originating from proteins like the viral TAT protein that are able to cross biological barriers. The CPPs uptake mechanism is highly debated and is thought to involve mainly the endocytic pathway. Trapping the conjugated cargo in endosomes, eventually landing in lysosomes where common enzymatic degradation mechanisms take place, often leads to a limited delivery of therapeutic agents to targets (Choi and David, 2014).

Hydrophobic peptides, that efficiently traverse biological membranes, promote lipid–membrane reorganizing processes and involve temporary membrane destabilization (Galdiero et al., 2014, 2015, 2012; Falanga et al., 2009), are able to avoid endosomal entrapment either favouring the escape from the endosome or by translocating directly into the cytosol, thus favouring energy independent processes. This idea has been exploited to design the drug delivery tool called gH625 (Galdiero et al., 2015; Valiante et al., 2015), which can be efficiently linked to different potential therapeutic molecules and/or nanovectors and represents an extremely powerful tool to increase their uptake. gH625 is a peptide derived from glycoprotein H of Herpes simplex virus type I, which has been shown to have many applications, from membrane fusion (Galdiero et al., 2005), to viral inhibition (Galdiero et al., 2008; Tarallo et al., 2013) and drug delivery (Galdiero et al., 2012). gH625 has the ability to penetrate deep into the bilayer as a helix without causing significant bilayer perturbations. This ability may help explaining its translocation

across the bilayer. It has been recently demonstrated that gH625 is able to transport into the cytosol several compounds, such as quantum dots (QDs) (Falanga et al., 2011), liposomes (Tarallo et al., 2011), nanoparticles (NPs) (Guarnieri et al., 2013), dendrimers (Carberry et al., 2012; Falanga et al., 2014), and proteins (Smaldone et al., 2013).

The cellular uptake of liposomes or other nanosystems decorated on their surface with gH625 has been previously determined by flow cytometry (Fluorescence-activated cell sorting – FACS) and confocal fluorescence microscopy (Falanga et al., 2011; Tarallo et al., 2011). It has been shown that the mechanism of nanosystem uptake could be modified by the presence of the peptide and that the internalization of functionalized nanosystems is mainly not energy-dependant. However, the analysis was limited to the overall detection of the drug used and did not account for the subcellular fluorescence changes, depending on the drug environment/interaction. Confocal spectral imaging (CSI) represents an alternative technique based on measurement, at different points of a cell, of the fluorescence spectra, which provides the opportunity to distinguish different molecular states of the intracellular drug (Sharonov et al., 1994). Thus, CSI is a powerful tool for mapping the MTX molecular interactions within compartments of living cells.

In this work, in order to get a better insight into the role of gH625 on the mechanism of liposome-mediated drug delivery, we have performed a comparative study of HeLa cells treated with MTX-loaded PEGylated liposomes (LMTX) and from LMTX functionalized with gH625 (LMTX-gH625). Prior to cellular experiments, the liposomes were carefully characterized in terms of their physical properties (hydrodynamic size, surface charge), chemical composition (MTX content, gH625 conformation) and drug release kinetics. Both the FACS data on the quantity of total intracellular MTX, the CSI data on the subcellular drug distribution/interaction and the cytotoxicity assay data indicate that the functionalization of liposomes with the peptide gH625 affects the drug delivery qualitatively and quantitatively.

2. Material and methods

2.1. Materials

Fmoc-protected amino acid derivatives, coupling reagents, and Rink amide *p*-methylbenzhydrylamine (MBHA) resin were purchased from Calbiochem-Novabiochem (Laufelfingen, Switzerland). Fmoc-L-propargylglycine (Fmoc-Pra-OH) was purchased from Polypetide (Strasbourg, France). Mitoxantrone and other chemicals were purchased from Sigma–Aldrich, Fluka (Buchs, Switzerland), or LabScan (Stillorgan, Ireland) and were used as received, unless otherwise stated. 1,2-Dioleoyl-*sn*-glycero-3-phosphocholine (DOPG) and 1,2-distearoyl-*sn*-glycero-3-phosphoethanolamine-*N*-[amino(polyethylene glycol)-2000] (ammonium salt) were purchased from Avanti Polar Lipids (Alabaster, AL). HeLa, cervical cancer cell of an African–American woman was purchased from ATCC, Rockille, (MD, USA), Dulbecco's Minimal Essential Medium was obtained from Gibco, Invitrogen Co. (Carlsbad, CA, USA), foetal bovine serum was obtained from Euroclone, Milan, Italy, 100 mg/ml sodium pyruvate, 100 g/ml of nonessential aminoacids, 100 g/ml penicillin/streptomycin and 100 U/ml glutamine was bought from Invitrogen Life Technologies, Italy and Hank's Balanced Salt Solution from Fisher Bioblock Scientific, Illkirch, France. Other reagents were all of analytical grade.

2.2. Solid-phase peptide synthesis

gH625 was synthesized using standard solid-phase 9-fluorenylmethoxycarbonyl (Fmoc) procedures with a Syro I

MultiSynThec GmbH (Wullener, Germany) automatic synthesizer, as previously reported (Galdiero et al., 2005).

The Rink amide MBHA resin (substitution 0.51 mmol/g) was used as the solid-phase support, and syntheses were performed on a scale of 20 μmol. The peptide was synthesized by consecutive deprotecting and coupling step. Coupling: Fmoc-protected amino acids (4 equivalents relative to resin loading) HBTU (0.5 M in DMF, 4 equiv), HOBt (0.5 M in DMF, 4 equiv), and DIPEA (2 M in DMF, 8 equiv). Deprotection: 30% piperidine in DMF (v/v).

The gH625-Pra was synthesized to allow binding to preformed-liposomes. Fmoc-Pra-OH was coupled once for 45 min with 2 equivalents of PyBop/HOBt and 4 equivalents of DIPEA. The peptide was fully deprotected and cleaved from the resin with a solution of TFA/water/anisole/thioanisole 93.5/2.5/2.0/2.0, at room temperature for 300 min. Then, it was precipitated with ice-cold ethyl ether, filtered, dissolved in water, and lyophilized. Purification was performed by RP-HPLC on a LC8 Shimadzu HPLC system (Shimadzu Corporation, Kyoto, Japan) equipped with a UV lambda-Max Model 481 detector using a Phenomenex (Torrance, CA) C_{18} (300 Å, 250 × 21.20 mm, 5 μ) column eluted with H_2O/0.1% TFA (A) and CH_3CN/0.1% TFA (B) from 20 to 80% over 20 min at a flow rate of 20 ml/min. Purity and identity were assessed by analytical LC–MS analyses using a Finnigan Surveyor MSQ single quadrupole electrospray ionization (Finnigan/Thermo Electron Corporation, San Jose, CA), column: C_{18}-phenomenex eluted with H_2O/0.1% TFA (A) and CH_3CN/0.1% TFA (B) from 20 to 80% over 10 min at a flow rate of 0.8 ml/min. The final yield of purified peptide ranged between 30 and 40%. Azide-AdOO-Lys(C(O)CH$_2$CH$_2$C(O)N-$(C_{18}H_{37})_2$)-amide (($C_{18})_2$L-N_3) monomer was synthesized on solid phase under standard conditions using the Fmoc/tBu strategy as previously reported (Tarallo et al., 2011).

2.3. Liposomes preparation

Liposomes were prepared by the thin lipid film hydration procedure. Mixed aggregates of DOPG/DSPE-PEG/$(C_{18})_2$L-N_3 (85:5:10 molar ratio) were prepared by dissolving the lipids in a small amount of chloroform, and subsequently evaporating the solvent by slowly rotating the tube containing the solution under a stream of nitrogen and eventually lyophilized overnight. A thin film of amphiphiles was obtained. The dry lipid film was suspended in HEPES–NaCl buffer (5 mM–100 mM) at pH 7.4 by vortexing; then the lipid suspension was freeze–thawed ten times and extruded ten times thought a polycarbonate membrane with 100 nm pore size using a thermobarrel extruder (Northern Lipids Inc., Canada).

2.4. Functionalization of liposomes with gH625

The click reaction was carried out on DOPG/DSPE-PEG/$(C_{18})_2$L-N_3 liposomes adding CuSO$_4$·5H$_2$O (4.4 equiv), ascorbic acid (6.7 equiv), and the peptide derivative (1 equiv) with respect to the azido moiety. In particular, solutions containing CuSO$_4$·5H$_2$O (60.5 mM, solution A), ascorbic acid (81.4 mM, solution B), and the alkyn-modified peptide (1 mM, solution C) were freshly prepared in water.

Solution A (11.6 μl), solution B (13.2 μl), and solution C (145.4 μl) were added to a suspension of azido-functionalized preformed liposomes in HEPES–NaCl buffer (400 μl). The concentration of solution C was determined measuring the tryptophan absorbance at 280 nm on a UV/vis Jasco V-5505 spectrophotometer.

The reaction mixture was stirred at 40 °C for 30 min and then left overnight at room temperature. After the conjugation step the liposomes were purified by exclusion chromatography on a 1 × 18 cm Sephadex G-50 (Amersham Biosciences) column pre-equilibrated with HEPES buffer.

2.5. MTX encapsulation in liposomes

MTX was remote-loaded in DOPG/DSPE-PEG/$(C_{18})_2$L-N_3 liposomes through an ammonium sulphate gradient method. Briefly, a liposomal solution was prepared as reported above in an ammonium sulphate solution (250 mM) at pH 5.5. Next, the external buffer was removed by ultra centrifugation at 151,332 × g, at 4 °C for 3 h, and the liposomes were resuspended in 400 μl of HEPES–NaCl buffer (5 mM–100 mM) at pH 7.4. A MTX solution (18 μl at 2 mg/ml) in water was added to the liposomal solution, to achieve a final lipid to drug weight ratio of 10:1. This suspension was stirred for 30 min at 60 °C. Unloaded MTX was removed with a Sephadex G50 column for determination of entrapment efficiency. The MTX concentration was determined by UV spectroscopy measuring the drug absorbance at λ = 655 nm. The Drug Loading Content (DLC, defined as the weight ratio of encapsulated drug vs the amphiphilic moieties) was quantified by subtracting the amount of MTX removed from the total amount loaded. Finally, the MTX pre-loaded liposomes were modified with gH625 by using the click-chemistry reaction procedure, as reported above.

2.6. Quantification of MTX loaded into the liposomes

The presence of copper in Lipo-MTX-gH625 determines the formation of a complex between copper and MTX which quenches fluorescence and absorbance of the drug. In order to verify that the quantity of MTX in both liposomes conjugated or not with the peptide were equal, both preparations were treated with 0.2% Triton X-100 and then with EDTA (10 mM, 91 μl) with incubation for 1 h at 37 °C. Finally, the drug absorbance measured at 655 nm was used to determine its concentration according to the previously established calibration curve.

2.7. Particle size and zeta potential analyses

The hydrodynamic diameter (D_H) and the polydispersity index (PDI) of LMTX and LMTX-gH625 were measured using dynamic light scattering (DLS) method (Malvern Nanosizer Nano ZS, Malven, UK). The zeta potential was determined using Malvern Nanosizer NanoZS (Malvern, Malven, UK). The instrument use a He–Ne laser 4 mW source operating at 633 nm with the scattering angle fixed at 173°. Each measurement was performed at 25 °C, at least in triplicate.

2.8. gH625 conformation monitoring by circular dichroism (CD)

CD spectra in the range from 260 to 195 nm were recorded with a Jasco J-810 spectropolarimeter equipped with a NesLab RTE111 thermal controller unit. For the measurements, liposomes decorated with gH625 were diluted 10 times in a H_2O and placed in a 10 mm quartz cellstabilized at 25 °C. Other experimental settings were: scan speed of 10 nm min^{-1}, sensitivity of 50 m deg, time constant of 16 s, bandwidth of 1 nm. Each spectrum was obtained through averaging three scans, subtracting the contributions from other species present in solution, and converting the signal to mean molar ellipticity.

2.9. In vitro drug release

The in vitro release kinetics of MTX from liposomes was determined using UV–vis spectrophotometry. LMTX and LMTX-gH625 at equivalent MTX concentration were placed into 2 ml of HEPES–NaCl buffer and into under continuous stirring at 37 °C. The release studies were carried out in triplicate. At predetermined time intervals, 200 μl aliquots were withdrawn and replaced with equal volume of fresh medium. The free drug was collected by a

Sephadex G50 column and MTX was quantitated based on the UV–vis absorbance at 655 nm using a previously established calibration curve. The cumulative amount of MTX released over 24 h was quantified, and results were plotted against incubation time.

2.10. In vitro cytotoxicity studies

The estimation of cell viability was performed by staining with Trypan Blue (TB) (Invitrogen). This marker, added to a cell suspension, is able to cross cell membranes that have been changed significantly. The TB penetrates only into damaged cells giving them a blue colour observable under an optical microscope. The viable cells, which are not permeable to the marker, remain colourless. This assay was performed on HeLa, cervical cancer cell of an African–American woman (ATCC, Rockille, MD, USA, CCL-2) grown as monolayers in Dulbecco's Minimal Essential Medium (Gibco BRL, Invitrogen Corporation, Carlsbad, CA, USA), supplemented with 10% foetal bovine serum (FBS – Euroclone, Milan, Italy), 100 mg/ml sodium pyruvate, 100 g/ml of nonessential aminoacids, 100 g/ml penicillin/streptomycin and 100 U/ml glutamine (Invitrogen – Life technologies, Italy). These cells were cultured at 37 °C, in a humidified incubator in presence of 5% CO_2, using sterile flasks. After reaching the confluence of the flask, the medium was removed and the cells were washed with phosphate buffer saline (PBS). Subsequently, the cells were incubated with a solution of trypsin (0.05% trypsin, 0.0022% EDTA) and PBS at 37 °C in the presence of 5% CO_2 for 3 min. Finally, the cells detached from the flask were transferred into a sterile tube (Falcon) and centrifuged at $325 \times g$ for 10 min. The cell pellet obtained was resuspended in fresh culture medium and the cells were seeded in 12 well plates (Falcon) in complete medium at a concentration of 350.000–400.000 cells/well. The following day, the cells were treated with different concentrations of LMTX and LMTX-gH625; controls were used as untreated cells (negative control) and cells treated with H_2O_2 (positive control). At the end of the treatments of 1, 4, 6, 12, 24, 48 and 72 h, the cells were washed three times with PBS to remove the liposomes in excess, and then trypsinized. The cells completely detached were transferred in falcon tubes and 25 μl of the cell suspension were mixed with 475 μl of TB. The cells were counted using the appliance Countess® Cell Counter (Invitrogen). The results were expressed as percentage of control.

2.11. In vitro cellular uptake by flow cytometry

The cellular uptake of MTX-loaded liposomes was analysed by flow cytometry. HeLa cells, cultured in Dulbecco's Minimal Essential Medium supplemented with 10% foetal bovine serum, were seeded into six-well at a density of 3×10^5 cells/ml at 37 °C for 48 h. Then, cells were treated with a final concentration of 5 μM of LMTX and LMTX-gH625 in PBS medium for 1 and 4 h in a volume of 1 ml. Thereafter, cells were washed three time, trypsinized, harvested and then resuspended in 0.5 ml of PBS. The MTX fluorescence associated to the cells was measured by FACs analysis (BD Accuri), using FL4 channel 675/25 nm. The events collected were ten thousand and BD Accuri C6 software was used to calculate mean fluorescence intensity (MFIs) for each sample. MFIs values were reported as histogram.

2.12. In vitro cellular uptake and distribution by confocal spectral imaging (CSI)

HeLa cells were plated at a density of 4×10^4 cells/well in 24-well plates onto cover glasses for 48 h in DMEM media supplemented with 10% serum. HeLa cells were then incubated with either LMTX or LMTX-gH625 at drug concentration of 1 μM for 1 and 4 h at 37 °C in DMEM media without serum. After the

incubation with the liposomes, the medium was removed and the cells were washed three times with fresh HBSS (Hank's Balanced Salt Solution, Fisher Bioblock Scientific, Illkirch, France). Washed cells were placed between slide and slip cover. Fluorescence measurements were carried out using a LabRAM confocal microspectrometer (Horiba, Villeneuve d'Ascq, France). The MTX fluorescence was excited with a 632.8 nm line of an internal, air-cooled, helium–neon laser. The power on the samples was ∼30 μW, the acquisition time was 0.02 or 0.05 s/spectrum. After the acquisition, all the spectra were normalized to an intensity corresponding to the same acquisition duration. Treatment of spectral maps was made using LabSpec 4.18 software (Horiba Villeneuve d'Ascq, France).

3. Results

3.1. Physico-chemical properties of liposomes

3.1.1. Synthetic components

The liposome component $(C_{18})_2L-N_3$ and the peptide gH625 bearing a propargylglycine moiety (gH625-Pra) were synthesized by the standard solid phase peptide synthesis (SPPS) protocols with Fmoc/tBu (tBu = tert-butyl) chemistry. The alkyne moiety was introduced at the C-terminus of the peptide as an L-propargylglycine. The compounds identity and the purity were confirmed by mass spectrometry, ^{1}H and ^{13}C NMR spectroscopy (for $(C_{18})_2L-N_3$), and LC–MS (Tarallo et al., 2011). Both gH625-Pra and $(C_{18})_2L-N_3$ were collected in good yields (30–40% and 85%, respectively) after HPLC-RP purification.

3.1.2. Blank liposomes

Liposomes coated with PEG (DOPG/DSPE-PEG/$(C_{18})_2L-N_3$liposomes) were generated according to classical procedures (Hope et al., 1985). Briefly, the lipid mixture was dissolved into ammonium sulphate buffer and then the suspension was extruded ten times through a polycarbonate membrane (100 nm).

3.1.3. MTX-loaded liposomes

To obtain the MTX-loaded liposomes (LMTX) we used the well-assessed procedures based on an ammonium sulphate gradient (Tardi et al., 1996); in particular, a solution containing MTX was incubated with liposomes under stirring for 30 min at 60 °C. Subsequently, unloaded MTX was removed using a Sephadex G50 column pre-equilibrated with HEPES–NaCl buffer (5 mM–100 mM) at pH 7.4. The drug/lipid weight ratio chosen
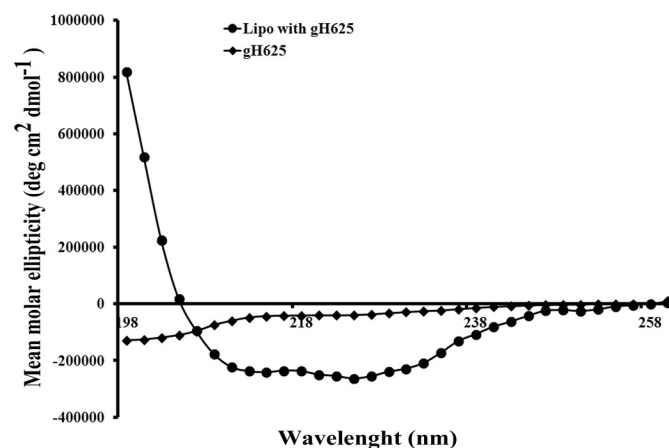

Fig. 1. Circular dichroism spectrum of gH625 conjugated to blank liposomes and of gH625 alone.

Table 1
Colloidal characteristics of LMTX and LMTX-gH625.

Liposome type	Hydrodynamic diameter, nm	Polydispersity index	Zeta potential, mV
LMTX	111.80 ± 1.42	0.09 ± 1.01	−26.30 ± 1.01
LMTX-gH625	122.00 ± 1.05	0.19 ± 0.07	−21.30 ± 1.10

Data obtained for three independently prepared batches of each liposome type, with atlease 13 runs per batch.

for the loading experiments was 0.1. The resulting LMTX were used as it or were modified with the gH625-Pra peptide (to become LMTX-gH625) *via* click-chemistry reaction performed in aqueous medium. The coupling of the Pra moiety of the gH625 to the liposomes surface was obtained due to a copper(I)-catalyzed Huisgen 1,3-dipolar cycloaddition reaction of azides and alkynes (Said Hassane et al., 2006). Cu(I) catalyser was generated *in situ* by reduction of $CuSO_4$ with ascorbic acid (Sharma and Sharma, 1997). The LMTX-gH625 were obtained with a yield higher than 90% after 12 h at room temperature. Circular dichroism (CD) spectra showed that gH625 when conjugated to liposomes at a concentration of 1.25×10^{-6} M adopts an α helical conformation (Fig. 1), while the peptide alone in buffer adopts a random coil structure; suggesting that the coupling on the surface of the liposomes was sufficient to induce the secondary structure which is probably playing a key role in translocation across the membrane bilayer.

Dynamic light scattering (DLS) data on LMTX and on LMTX-gH625 dispersed in aqueous medium at pH 7 (Table 1) showed that the liposome functionalization with gH625 only slightly increased their average hydrodynamic diameter, from *ca.* 112 to 122 nm. The polydispersity index changed from *ca.* 0.09 to *ca.* 0.19, indicating that the distribution of the liposome size remained rather narrow and there are no signs of aggregation. These parameters should favour both the effective extravasation of liposomes and their longer retention in tumour tissues.

The surface charge of the liposomes, as determined by measurement of their zeta potential, was also slightly reduced on going from LMTX to LMTX-gH625, from *ca.* −26 to −21 mV (Table 1). It is widely accepted that at high values of ξ-potential (over 20 mV, positive or negative) the electrostatic repulsions between particles are strong enough to ensure their colloidal stability. At smaller values of ξ-potential, particles can flocculate, except if they have sterical repulsion like in the case of PEG coating. Anyhow, the aqueous suspensions of both LMTX and LMTX-gH625 appear as stable colloids.

3.1.4. MTX loading efficiency and release kinetics

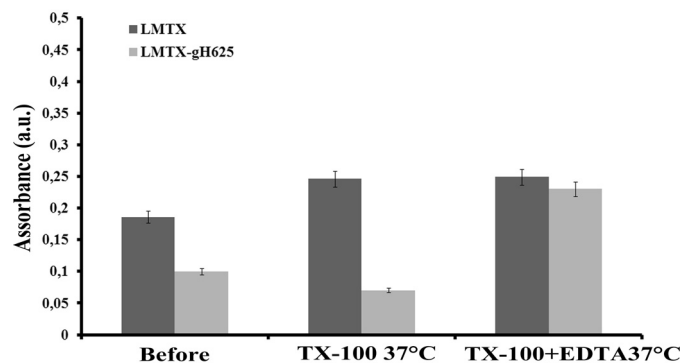The drug loading efficiency calculated from the unloaded MTX absorbance at $\lambda = 655$ nm was found at least as high as 97% of the total amount incubated and it was nearly the same in both LMTX-gH625 and LMTX.

In spite of the same concentration inside the liposomes, the MTX fluorescence intensity from LMTX in aqueous suspension was about 5.7 times higher than in LMTX-gH625. The MTX fluorescence in gH625 should be partially quenched by Cu ions used to catalyse the peptide coupling to the liposomes. This hypothesis was confirmed by the experiment described below. Both LMTX and LMTX-gH625 were dissolved by treatment with 0.2% of Triton X-100 and incubation for 1 h with EDTA (10 mM) at 37 °C. This treatment brought to a full restoration of MTX absorbance intensity of MTX released from LMTX-gH625, while for LMTX, which did not contain copper, the absorbance intensity of the released drug was not affected (Fig. 2). Therefore, copper ions are able to penetrate LMTX-gH625 and to quench there the loaded MTX fluorescence and absorbance; however, once the drug escapes from the liposomes, the quenching is no more active.

There were no pronounced differences between LMTX and LMTX-gH625 from the point of view of the drug release kinetics *in vitro*, in HEPES–NaCl buffer (Fig. 3). Less than 30% of loaded MTX was released within 24 h, indicating the good stability of liposomes.

3.2. Biological activity of LMTX and LMTX-gH625 in HeLa cells in vitro

The cytotoxicity of liposomes was evaluated staining Triptan Blue on HeLa cells. Within 4 and 6 h treatment duration, cytotoxicity was higher for LMTX-gH625 than LMTX (Fig. 4a). At 48 and 72 h we did not notice significant differences between the two types of liposomes; indicating that at high incubation times both are significantly toxic to the cells. We thus selected 1 and 4 h for further experiments as these were more representative of the differences between the two nanosystems.

Flow cytometry allowed us to compare quantitatively the MTX uptake by HeLa cells treated with LMTX-gH625 or with LMTX (Fig. 4b). We clearly observed an increased uptake of MTX from liposomes decorated with gH625.

For better understanding of the observed cytotoxicity and uptake details, we determined the subcellular distribution and interaction of the delivered MTX in live HeLa cancer cells using confocal spectral imaging (CSI) technique. As described above, the
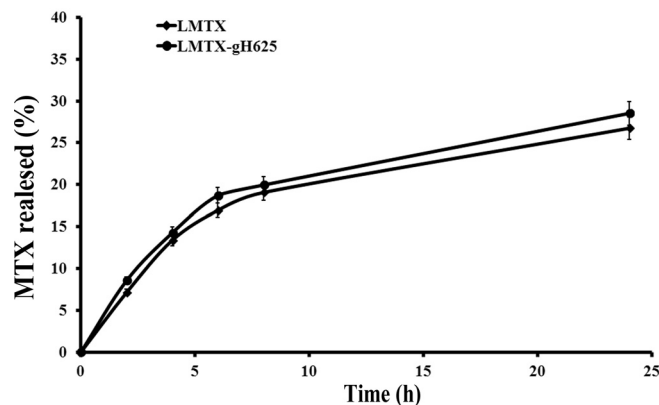

Fig. 2. Effect of combination of Triton and EDTA on LMTX and LMTX-gH625. Both liposomes were treated by Triton X-100 (TX-100) and 10 mM of EDTA at 37 °C. The presence of EDTA brought full restoration of MTX absorbance intensity in LMTX-gH625, while on LMTX had not effect.

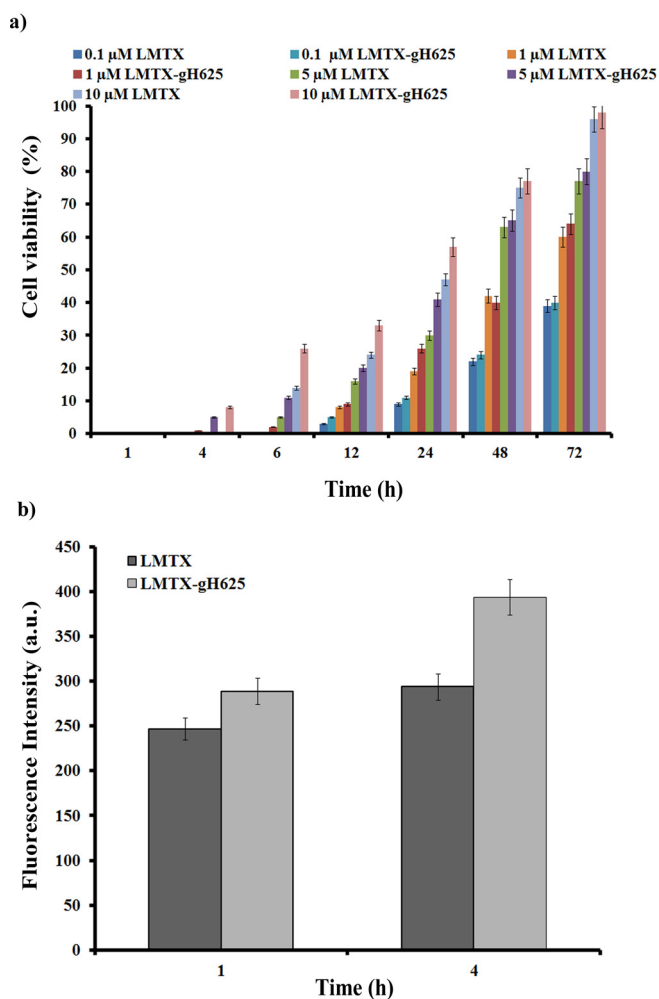**Fig. 3.** Kinetics of *in vitro* release of MTX from LMTX and LMTX-gH625.

Fig. 4. Cytotoxicity of liposomes on HeLa cells at several times of incubation (panel a). Flow cytometry data on the MTX uptake by HeLa cells (panel b).

CSI approach consists in recording the complete fluorescence at each scanned point of the cell and therefore exploiting both the spectral shape and intensity.

Full fluorescence spectra (in the 640–920 nm range) were then recorded *via* point-by-point scanning of the equatorial optical section of the treated cells (see material and methods). From these spectra, the parametric maps were generated using either total fluorescence intensity (area of the whole spectrum) or coefficients determined from fitting each experimental spectrum with spectra characteristic of 3 intracellular molecular interactions of the drug: (i) MTX at lipophilic environment, where the spectrum is very close in shape to that of the drug in LMTX in suspension (blue zones and spectra in Fig. 5); (ii) MTX in nucleus, where a significant bathochromic shift of the spectrum is observed due to the drug intercalation between DNA base pairs (green zones and spectra); and (iii) an oxidative metabolite of the drug stained in the low polarity environment, with the blue-shifted spectrum (red zones and spectra). These characteristic spectra are consistent with those we previously reported for the MTX incubated as aqueous solution to MDA-MB-231 and MCF-7 cancer cell lines (Vibet et al., 2007).

In the present study, the fact that not only the blue spectra but also the shifted ones were observed indicates that the drug was released, at least in part, from the liposomes and was able to reach the nucleus. Interestingly, the blue and red spectra were highly co-localized in some perinuclear regions, indicating that the lipophilic locations favour the drug oxidative metabolism. In our

previous study (Vibet et al., 2007), we found the metabolite to be co-localized with the fluorescent label of endoplasmic reticulum and its presence correlated with higher sensitivity of cancer cells to chemotherapeutic drug MTX. From the point of view of the fluorescence intensity, it is difficult to establish the exact quantum yields (QY) in these three subcellular situations. Nevertheless, it is commonly believed that the lower polarity environment of fluorophore favours higher QY, while the DNA intercalation leads to a partial quenching of the drug fluorescence. In this consideration, the intensities used in Fig. 5 allow only a comparative discussion, but could be calibrated to concentrations once the QY are established (it was not a subject of the present study).

The results shown in Fig. 5 allow to analyse two effects, that of incubation duration (1 h *vs* 4 h) and that of the liposomes functionalization with gH625. The spectral maps show that the increase of the incubation duration from 1 h to 4 h, determines a significant increase of the total intracellular drug fluorescence (2–5 fold, see the statistical summary in Fig. 5). Similar total fluorescence intensity was reached with both types of nanosystems. In contrast, for the LMTX and not for the LMTX-gH625, 4 h *vs* 1 h incubation resulted in a subcellular redistribution of the MTX fluorescence: the relative fractions of lipophilic *vs* nuclear locations were inversed. The analyses of this inversion together with the nearly 2-fold increase of total intensity in LMTX between 1 and 4 h, leads one to the supposition that the total drug in the nucleus is probably not decreased while the drug presence in the perinuclear locations is more pronounced. For the LMTX-gH625, the drug fluorescence from the hydrophobic perinuclear regions was dominant even after only 1 h of incubation and the subcellular distribution remained nearly constant between 1 h and 4 h of incubation. The latter means that the 5-fold increase of the intracellular fluorescence intensity for the gH625-modified liposomes is related to the increased uptake of the liposomes and not to the QY changes.

The subcellular distribution of MTX delivered with liposomes was different from that of MTX in solution: while the drug solution was mainly and rapidly stained in nucleus of cancers cells (Vibet et al., 2007), liposomes mainly directed the drug to the perinuclear zones where the metabolite production/staining by the cells was also more significant than with solutions. This could be the effect of the liposomal delivery of MTX.

The above described results lead to the following conclusions about the effect of the liposomes functionalization with gH625: (i) it makes the MTX uptake to the hydrophobic perinuclear staining zones even more efficient; (ii) it favours even more the presence of an oxidative metabolite of the drug in the same perinuclear regions.

4. Discussion

Cell penetrating peptides (CPPs) have recently attracted much interest as very efficient agents to enhance drug delivery into target cells. Amongst the CPPs, gH625 represents a novel sequence with great possibility of overcoming the known limits of classical CPPs. In previous studies, we have demonstrated that gH625 acts as a potent vector for the cell delivery of molecules and nanosystems (Galdiero et al., 2015). It is widely accepted that drug intracellular distribution changes when they are bound to CPPs (Tarallo et al., 2011; Aroui et al., 2009). The clarification of the mechanism of internalization could be useful to improve the design of anticancer delivery tools that may determine an increase of internalization and may also help in overcoming resistance problems. The purpose of this study was to explore the possibility of using nanoliposomes decorated on their external surface with a novel CPP gH625 to change and enhance the internalization of MTX. We used CSI to distinguish very fine
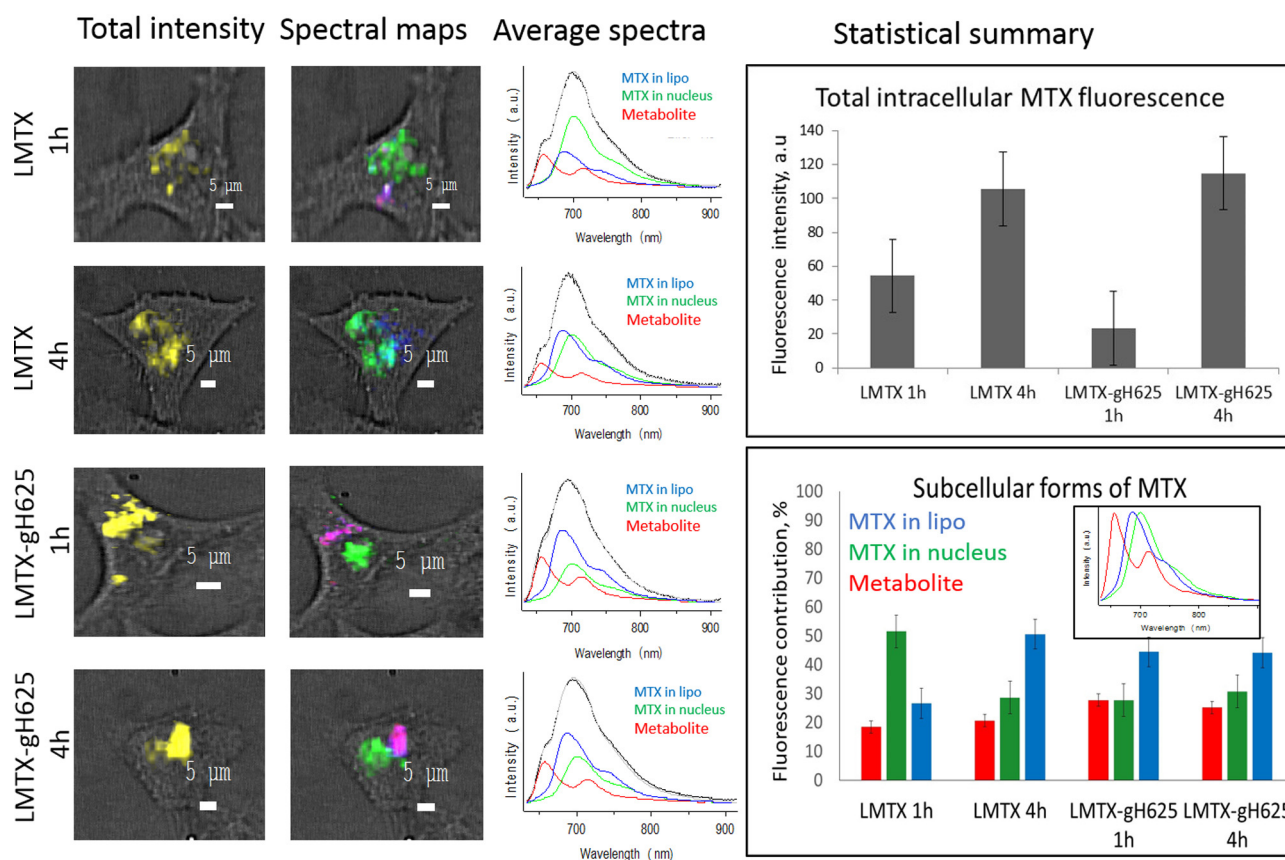
Fig. 5. *In vitro* study of subcellular interaction and distribution of MTX delivered from LMTX and LMTX–gH625 to live HeLa cancer cells. Left panel: representative images of individual cells, *i.e.* merge of the white light images with the fluorescence spectral maps showing either total spectral intensity (yellow zones) or merged spectral maps characteristic of 3 intracellular molecular interactions of the drug: MTX at lipophilic environment (blue zones and spectra), MTX-DNA complex in nucleus (green zones and spectra) and presence of an oxidative metabolite of the drug (red zones and spectra). Average spectra of the respective cells are shown in the middle column. Right panel: statistical summary of the data over a population of at least 6 cells. (For interpretation of the references to colour in this figure legend, the reader is referred to the web version of this article.)

modifications of MTX intrinsic fluorescence within different intracellular microenvironments.

The obtained results clearly show that the presence of gH625 on the surface of liposomes is favouring their uptake in HeLa cells: in fact, a greater quantity of MTX is internalized (Fig. 4b). This correlates well with toxicity data (Fig. 4a). Within 4 h, the LMTX–gH625 was more active than LMTX. The gH625 peptide probably induced a greater and more rapid internalization, which could contribute to the earlier cytotoxicity of LMTX–gH625 compared to LMTX. It has also been reported in literature that a fast cytoplasmic delivery of the drug can be related to a better chance to overcome drug resistance (Shen et al., 2009). Nevertheless at high incubation times there were no significant differences.

From the CSI spectra, we detected 3 intracellular molecular situation for the drug: MTX at lipophilic environment, MTX in nucleus and an oxidative metabolite of the drug stained in the low polarity environment. The spectra observed indicate that the drug was partially released from the liposomes and was able to reach the nucleus; moreover, the effect of gH625 consists also in an increased presence of an oxidative metabolite of the drug which we previously demonstrated to be correlated with sensitivity of cancer cells to chemotherapy by MTX (Vibet et al., 2007). We observed that Cu is able to lead to a partial fluorescence quenching for MTX loaded in LMTX–gH625. If we assume that a fraction of subcellular MTX found in lipophilic environment is still encapsulated in liposomes, it means that the real amount of internalized LMTX in presence of gH625 is even higher than what was estimated.

Our results support the view that, in addition to the nuclear one, several mechanisms may be involved in the cytotoxicity of LMTX–gH625 internalization.

5. Conclusions

The efficient passage of drugs across the cell membrane remains a major challenge for drug delivery. To address this need, CPPs seem promising as they can facilitate the entry of different covalently attached bulky cargo into cells without requiring specific receptors. However, the mechanism of internalization of these peptides is greatly dependant on the CPP used, the concentration, the type of cell line, and cargo carried. The uptake of CPPs is essentially mediated *via* endocytic pathways, although the exact mechanism of cellular uptake still remains controversial, and the endocytic uptake mechanism limits their use for drug delivery applications. gH625 is a membranotropic peptide derived from a viral fusion glycoprotein which is able to locally destabilize the membrane bilayer and thus cross the cell membrane with a mechanism which is essentially involving non-endocytic pathways. Previous studies allowed to verify that gH625 is able to modify the uptake mechanism of several nanosystems. Here, we further characterized this uptake mechanism and we found that gH625 modifies the internalization of liposomes and therefore the drug transport to the cells. Although the liposome-mediated drug delivery to the nucleus is delayed compared to the drug solution, it could be compensated by complementary mechanisms of cytotoxicity taking place into the cytosol, namely those involving

the oxidative metabolism of the drug. These mechanisms are of particular interest for the anticancer activity evaluation of the nanosystems for drug delivery. Our studies demonstrated that the cellular uptake of liposomes is significantly enhanced by the coupling of gH625 and the mechanism of uptake is modified. In the long run, we believe that the use of gH625 combined with the identification of the optimal sequences for targeting various cancers, will enable successful design of drug delivery platforms for the development of novel theranostic systems.

Acknowledgements

References

Aroui, S., Brahim, S., De Waard, M., Breard, J., Kenani, A., 2009. Efficient induction of apoptosis by doxorubicin coupled to cell-penetrating peptides compared to unconjugated doxorubicin in the human breast cancer cell line MDA-MB 231. Cancer Lett. 285, 28–38.

Carberry, T.P., Tarallo, R., Falanga, A., Finamore, E., Galdiero, M., Weck, M., Galdiero, S., 2012. Dendrimer functionalization with a membrane-interacting domain of herpes simplex virus type 1: towards intracellular delivery. Chemistry 18, 13678–13685.

Choi, Y.S., David, A.E., 2014. Cell penetrating peptides and the mechanisms for intracellular entry. Curr. Pharm. Biotechnol. 15, 192–199.

Cui, J., Li, C., Wang, C., Li, Y., Zhang, L., Yang, H., 2008. Repeated injection of pegylated liposomal antitumour drugs induces the disappearance of the rapid distribution phase. J. Pharm. Pharmacol. 60, 1651–1657.

Dawidczyk, C.M., Russell, L.M., Searson, P.C., 2014. Nanomedicines for cancer therapy: state-of-the-art and limitations to pre-clinical studies that hinder future developments. Front. Chem. 2, 69.

Dunn, C.J., Goa, K.L., 1996. Mitoxantrone: a review of its pharmacological properties and use in acute nonlymphoblastic leukaemia. Drugs Aging 9, 122–147.

Falanga, A., Cantisani, M., Pedone, C., Galdiero, S., 2009. Membrane fusion and fission: enveloped viruses. Protein Pept. Lett. 16, 751–759.

Falanga, A., Vitiello, M.T., Cantisani, M., Tarallo, R., Guarnieri, D., Mignogna, E., Netti, P., Pedone, C., Galdiero, M., Galdiero, S., 2011. A peptide derived from herpes simplex virus type 1 glycoprotein H: membrane translocation and applications to the delivery of quantum dots. Nanomedicine 7, 925–934.

Falanga, A., Tarallo, R., Carberry, T., Galdiero, M., Weck, M., Galdiero, S., 2014. Elucidation of the interaction mechanism with liposomes of gH625-peptide functionalized dendrimers. PLoS ONE 9, e112128.

Galdiero, S., Falanga, A., Vitiello, M., Browne, H., Pedone, C., Galdiero, M., 2005. Fusogenic domains in herpes simplex virus 1 glycoprotein H. J. Biol. Chem. 280, 28632–28643.

Galdiero, S., Falanga, A., Vitiello, M., D'Isanto, M., Cantisani, M., Kampanaraki, A., Benedetti, E., Browne, H., Galdiero, M., 2008. Peptides containing membrane-interacting motifs inhibit herpes simplex virus type 1 infectivity. Peptides 29, 1461–1471.

Galdiero, S., Vitiello, M., Falanga, A., Cantisani, M., Incoronato, N., Galdiero, M., 2012. Intracellular delivery: exploiting viral membranotropic peptides. Curr. Drug Metab. 13, 93–104.

Galdiero, S., Falanga, A., Vitiello, M., Grieco, P., Caraglia, M., Morelli, G., Galdiero, M., 2014. Exploitation of viral properties for intracellular delivery. J. Pept. Sci. 20, 468–478.

Galdiero, S., Falanga, A., Morelli, G., Galdiero, M., 2015. gH625: a milestone in understanding the many roles of membranotropic peptides. Biochim. Biophys. Acta 1848, 16–25.

Guarnieri, D., Falanga, A., Muscetti, O., Tarallo, R., Fusco, S., Galdiero, M., Galdiero, S., Netti, P.A., 2013. Shuttle-mediated nanoparticle delivery to the blood-brain barrier. Small 9, 853–862.

Heitz, F., Morris, M.C., Divita, G., 2009. Twenty years of cell-penetrating peptides: from molecular mechanisms to therapeutics. Br. J. Pharmacol. 157, 195–206.

Hope, M.J., Bally, M.B., Webb, G., Cullis, P.R., 1985. Production of large unilamellar vesicles by a rapid extrusion procedure: characterization of size distribution, trapped volume and ability to maintain a membrane potential. Biochim. Biophys. Acta 812, 55–65.

Kroger, N., Damon, L., Zander, A.R., Wandt, H., Derigs, G., Ferrante, P., Demirer, T., Rosti, G., 2003. Secondary acute leukemia following mitoxantrone-based high-dose chemotherapy for primary breast cancer patients. Bone Marrow Transplant. 32, 1153–1157.

Madni, A., Sarfraz, M., Rehman, M., Ahmad, M., Akhtar, N., Ahmad, S., Tahir, N., Ijaz, S., Al-Kassas, R., Lobenberg, R., 2014. Liposomal drug delivery: a versatile platform for challenging clinical applications. J. Pharm. Pharm. Sci. 17, 401–426.

Novak, R.F., Kharasch, E.D., 1985. Mitoxantrone: propensity for free radical formation and lipid peroxidation–implications for cardiotoxicity. Invest. New Drugs 3, 95–99.

Said Hassane, F., Frisch, B., Schuber, F., 2006. Targeted liposomes: convenient coupling of ligands to preformed vesicles using click chemistry. Bioconjugate Chem. 17, 849–854.

Sharma, A., Sharma, U.S., 1997. Liposomes in drug delivery: progress and limitations. Int. J. Pharm. 154, 123–140.

Sharonov, S., Chourpa, I., Morjani, H., Nabiev, I., Manfait, M., Feofanov, A., 1994. Confocal spectral imaging analysis in studies of the spatial distribution of antitumour drugs within living cancer cells. Anal. Chim. Acta 290, 40–47.

Shen, Y., Tang, H., Zhan, Y., Van Kirk, E.A., Murdoch, W.J., 2009. Degradable poly (beta-amino ester) nanoparticles for cancer cytoplasmic drug delivery. Nanomedicine 5, 192–201.

Smaldone, G., Falanga, A., Capasso, D., Guarnieri, D., Correale, S., Galdiero, M., Netti, P.A., Zollo, M., Galdiero, S., Di Gaetano, S., Pedone, E., 2013. gH625 is a viral derived peptide for effective delivery of intrinsically disordered proteins. Int. J. Nanomed. 8, 2555–2565.

Tarallo, R., Accardo, A., Falanga, A., Guarnieri, D., Vitiello, G., Netti, P., D'Errico, G., Morelli, G., Galdiero, S., 2011. Clickable functionalization of liposomes with the gH625 peptide from Herpes simplex virus type I for intracellular drug delivery. Chemistry 17, 12659–12668.

Tarallo, R., Carberry, T.P., Falanga, A., Vitiello, M., Galdiero, S., Galdiero, M., Weck, M., 2013. Dendrimers functionalized with membrane-interacting peptides for viral inhibition. Int J Nanomedicine 8, 521–534.

Tardi, P.G., Boman, N.L., Cullis, P.R., 1996. Liposomal doxorubicin. J. Drug Target. 4, 129–140.

Valiante, S., Falanga, A., Cigliano, L., Iachetta, G., Busiello, R.A., La Marca, V., Galdiero, M., Lombardi, A., Galdiero, S., 2015. The peptide gH625 enters into neuron and astrocyte cell lines and crosses the blood brain barrier in rats. Int J Nanomedicine 10, 1885–1898. doi:http://dx.doi.org/10.2147/IJN.S77734.

Vibet, S., Maheo, K., Gore, J., Dubois, P., Bougnoux, P., Chourpa, I., 2007. Differential subcellular distribution of mitoxantrone in relation to chemosensitization in two human breast cancer cell lines. Drug Metab. Dispos. 35, 822–828.

Wiseman, L.R., Spencer, C.M., 1997. Mitoxantrone. A review of its pharmacology and clinical efficacy in the management of hormone-resistant advanced prostate cancer. Drugs Aging 10, 473–485.